J Mater Sci: Mater Electron (2017) 28:1370–1377
DOI 10.1007/s10854-016-5670-3

Reduced dielectric loss and enhanced piezoelectric properties of Mn modified $0.71BiFeO_3$–$0.29BaTiO_3$ ceramics sintered under oxygen atmosphere

Qiang Li[1] · Jinrong Cheng[1] · Jianguo Chen[1]

Received: 12 August 2016 / Accepted: 29 August 2016 / Published online: 2 September 2016

Abstract $0.71BiFeO_3$–$0.29BaTiO_3$ piezoelectric ceramics with Mn modification (BF–BT–*x* %Mn) sintered in air and O_2 atmospheres have been investigated to understand the effects of sintering atmosphere on structure, dielectric, ferroelectric and piezoelectric properties. All ceramics exhibited the pseudo-cubic phase, while the O_2 sintered ceramics possessed larger grain sizes and more homogeneous distribution. Dielectric, ferroelectric and piezoelectric properties of BF–BT–*x*Mn ceramics were improved obviously after O_2 atmospheres sintering, especially for the compositions with Mn contents less than 1.2 mol%. The evidence of impedance spectroscopy indicated that the concentration of oxygen vacancies decreased significantly by the introduction of O_2 atmosphere. The dielectric loss $tan\delta$ was decreased down to 1/2 and the resistivity ρ enhanced 11 times for BF–BT–0 %Mn ceramics by the introduction of O_2 atmosphere. The strains of BF–BT–0.5 %Mn increased from 0.09 to 0.22 and the d_{33}^* increased from 119 to 284 pm/V after sintering in O_2 atmosphere. The Curie temperature and piezoelectric constant of O_2 sintered BF–BT–1.2 %Mn reached up to 500 °C and 353 pm/V, respectively. This work suggests that sintering in the O_2 oxygen atmosphere is an effective way to improve the dielectric and piezoelectric properties of $BiFeO_3$–$BaTiO_3$ solid solutions.

✉ Jianguo Chen
kpfocus@shu.edu.cn

[1] School of Materials Science and Engineering, Shanghai University, Shanghai 200072, China

1 Introduction

$BiFeO_3$–$BaTiO_3$ (BF–BT) solid solutions have been received much attention because of lead-free trait and high Curie temperature. The BF–BT system was considered as a new potential lead-free candidate for high temperature piezoelectric applications [1, 2]. However, the low resistivity caused by oxygen vacancies and valence fluctuation of iron ions (Fe^{3+} and Fe^{2+}) makes poling process difficultly and limits their device applications [3–5].

It was reported that Mn modification could reduce the leakage current of the BF–BT solid solutions [6–8] by restraining the conversion of $Fe^{3+} \rightarrow Fe^{2+}$. The sintering atmosphere also played an important role in the properties of $BiFeO_3$-based ceramics [8, 9]. Yao et al. reported that the Mn-doping $0.8BiFeO_3$–$0.2BaTiO_3$ ceramics sintered in O_2 atmosphere possessed the enhanced properties with piezoelectric constant $d_{33} = 125$ pC/N, remnant polarization $P_r = 25.1$ μC/cm^2 and high Curie temperature $T_C = 637$ °C, respectively. The Mn-modified 0.75BF-0.25BT system was prepared by Leontsev et al. sintered in O_2 atmosphere possessing $d_{33} = 116$ pC/N with $T_C = 619$ °C and the resistance enhanced from 2.7×10^7 to 7.6×10^{12} Ω. Zhu et al. studied the effect of O_2-sintered on DC resistivity of $0.67BiFeO_3$–$0.33PbTiO_3$ prepared by conventional solid state reaction, which the ceramics sintered in O_2 atmosphere shown improved resistivity. As reported in the literature, the piezoelectric properties of BF–BT solid solutions reached the maximum at Rhombohedral and Cubic phase boundary located at about BF of 0.7. However, there was little attention have been paid on the effects of sintering atmosphere on the microstructure, dielectric, ferroelectric and piezoelectric properties of BF–BT near the phase boundary ceramics with different Mn contents.

In this work, the $0.71BiFeO_3$–$0.29BaTiO_3$ ceramics with different Mn contents were prepared by traditional solid state reaction method. The ceramics were sintered under air and O_2 atmospheres at the same conditions (dwelling time and sintering temperature). The microstructure, dielectric, ferroelectric and piezoelectric properties of $0.71BiFeO_3$–$0.29BaTiO_3$ ceramics sintered under different atmospheres were investigated.

2 Experimental

The ceramics in the $0.71BiFeO_3$–$0.29BaTiO_3$-x mol% MnO_2 (BF–BT–x %Mn) binary system sintered in air and O_2 atmospheres were fabricated by conventional solid state reaction method, where $x = 0$, 0.3, 0.5, 0.8, 1.0, 1.2, 1.5, 1.8, 2.0. A stoichiometric amount of Bi_2O_3(99 %), Fe_2O_3(99 %), $BaCO_3$(99 %), TiO_2(99 %), MnO_2(99 %) were weighted based on the chemical formula for each composition, all the raw materials were first mixed thoroughly in the polyethylene jar with ethanol for 24 h with stabilized zirconia balls. After drying, the mixed powders were calcined in crucibles at 750 °C for 4 h. Then, the calcined powders were milled in ethanol again for 24 h to reduce the particle size. Finally, the powders were pressed into pellets with a diameter of 12 mm at 120 MP. The pellets were sintered at 1000–1100 °C for 2 h in air and O_2 atmospheres (O_2 flow was 200 ml/min) followed by furnace cooling to room temperature.

The phase of ceramics was analyzed by X-ray diffraction (XRD, Rigaku-D/MAX-2000) with Cu K_α radiation at room temperature. Scanning electron microscopy (SEM, Hatichi S-3400 N) was used to examine the fresh fracture surfaces microstructure. For dielectric and ferroelectric measurements, the sintered pellets were polished to 0.4 mm, and electroded with a post-fire silver paste. Dielectric properties measurements as a function of temperature were made using a computer controlled Agilent4294A impedance analyzer. For piezoelectric measurements, the BF–BT–xMn ceramics were poled in silicone oil under a DC electric field of 80 kV/cm at 100 °C for 30 min. The piezoelectric constant d_{33} was measured by a quasi-static piezoelectric meter (ZJ-2, Beijing Institute of Acoustics). The polarization versus electric field hysteretic loops was characterized by a ferroelectric test system Precision Premier II (Radiant Co.).

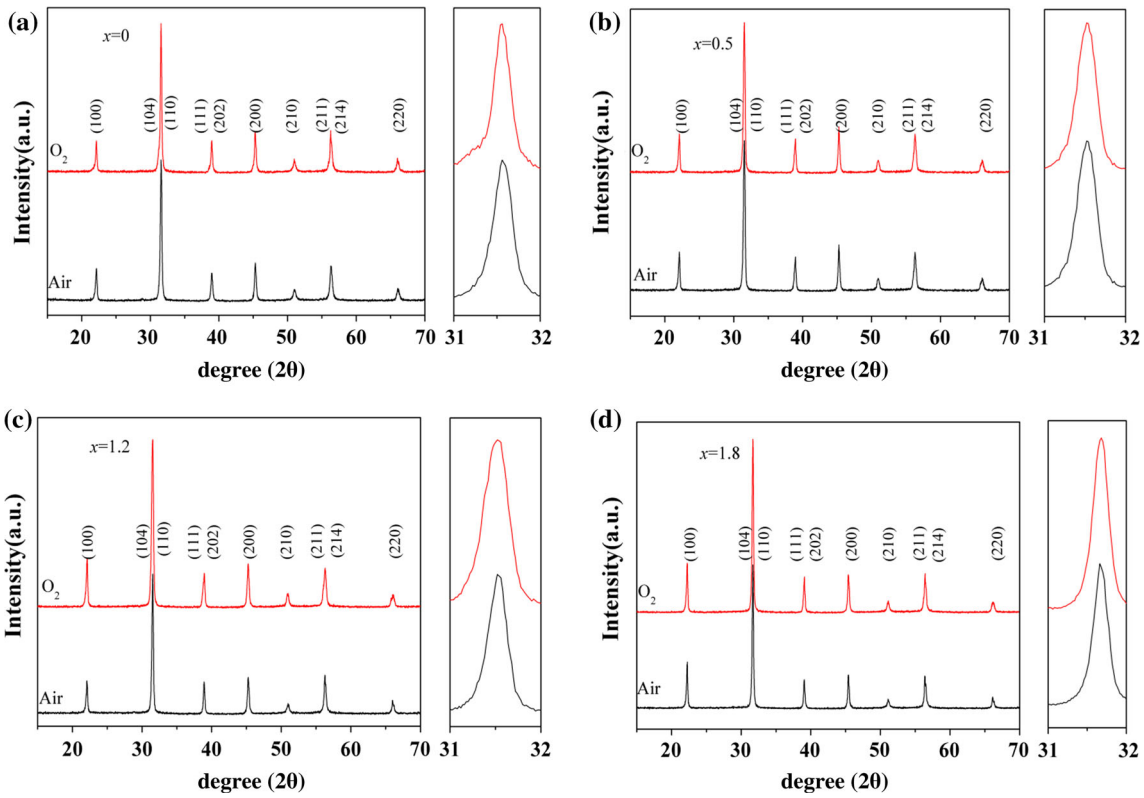

Fig. 1 XRD patterns of BF–BT–x %Mn ceramics sintered in air and O_2 atmospheres

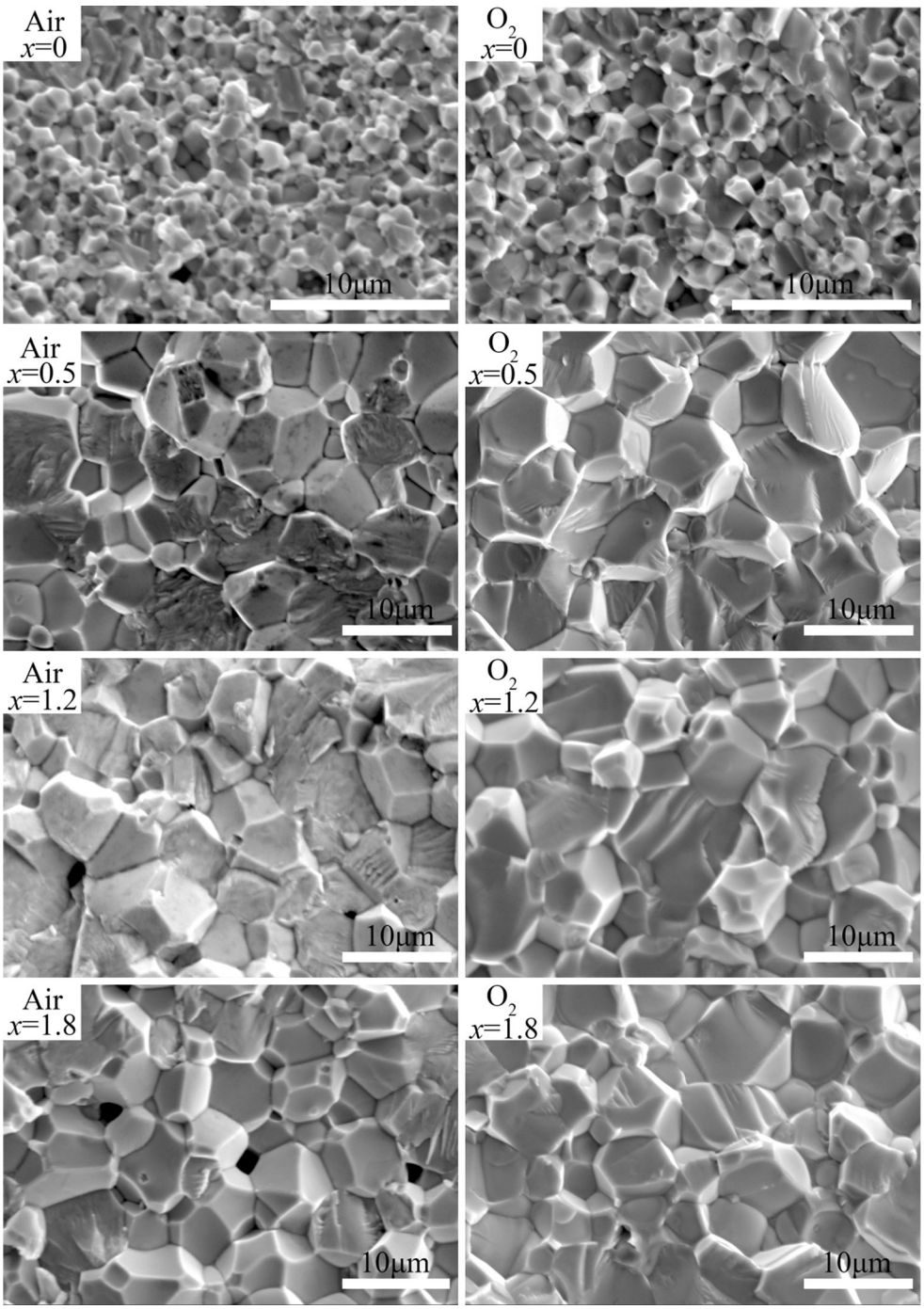

Fig. 2 SEM images of BF–BT–*x* %Mn ceramics sintered in air and O_2 atmospheres

3 Results and discussion

Figure 1 shows the XRD patterns of BF–BT–*x* %Mn ceramics sintered in air and O_2 atmospheres. All the XRD patterns exhibit a single perovskite structure without any secondary phases. BF–BT–*x* %Mn ceramics exhibit pseudo-cubic phase confirmed by XRD analysis, and there is no apparent phase difference between ceramics sintered in air and O_2 atmospheres. The diffraction peaks of O_2 sintered ceramics are sharper than that of air sintered ceramics indicating that better crystallinity was obtained.

Figure 2 presents the SEM images of BF–BT–*x* %Mn ceramics sintered in air and O_2 atmospheres derived from fresh fracture surfaces. The relative bulk density of air sintered ceramics is in the range of 93–96 %, while increase to 94–98 % for O_2 sintered ceramics. It can be

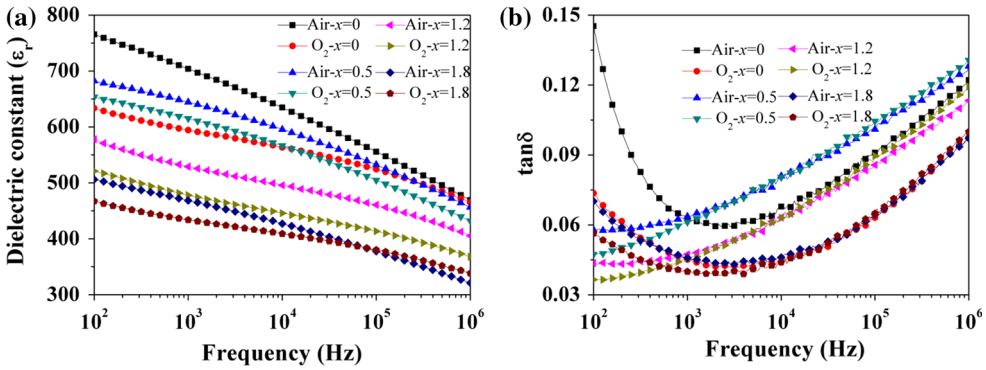

Fig. 3 Frequency dependence of ε_r and *tanδ* at room temperature for BF–BT–*x* %Mn ceramics sintered in air and O_2 atmospheres

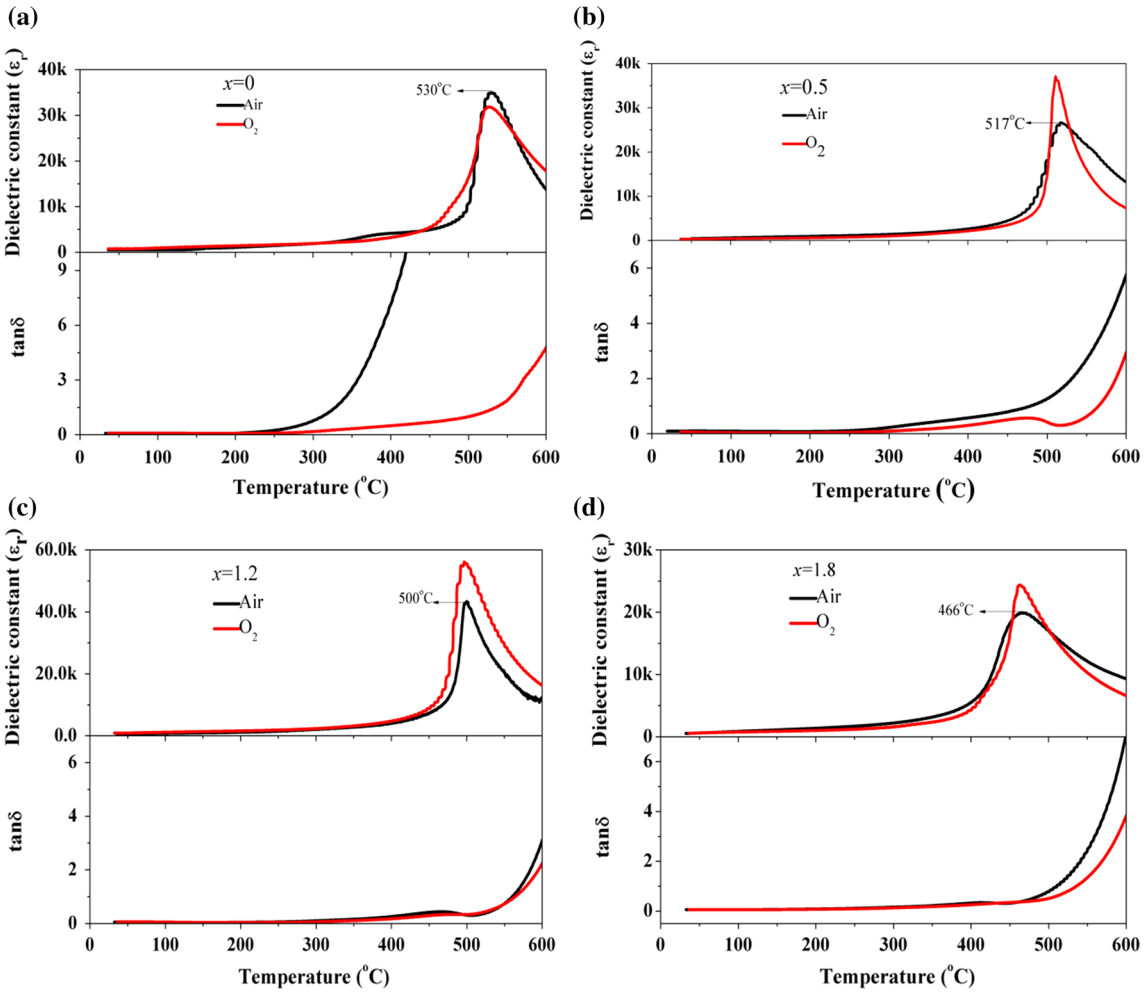

Fig. 4 The dielectric constant and loss of air and O_2 sintered BF–BT–*x* %Mn ceramics as a function of temperature at 10^6 Hz

found that the grain sizes of BF–BT–*x* %Mn ceramics sintered in O_2 atmosphere are more homogeneous and larger than that of air sintered ceramics, indicating that the O_2 atmosphere improves the rate of grain growth. The O_2 sintered ceramics possess better compactness by comparing the porosity, which may contribute to improving the dielectric, ferroelectric and piezoelectric properties.

Figure 3 depicts the variation of dielectric constant ε_r and dielectric loss *tanδ* for BF–BT–*x* %Mn ceramics sintered in air and O_2 atmospheres as a function of frequency. The values of ε_r for all BF–BT–*x* %Mn ceramics have a general tendency to decrease with the increasing frequency, which may result from space charge polarization due to the inevitable oxygen vacancies, A-site vacancies and the coexistence of Fe^{3+}/Fe^{2+} [10]. As shown in Fig. 3b, the *tanδ*

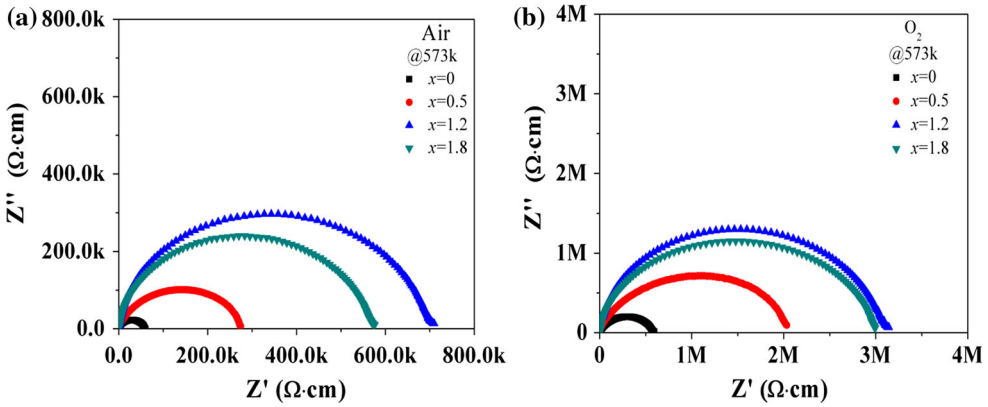

Fig. 5 Impedance spectroscopy of air and O_2 sintered BF–BT–*x* %Mn ceramics

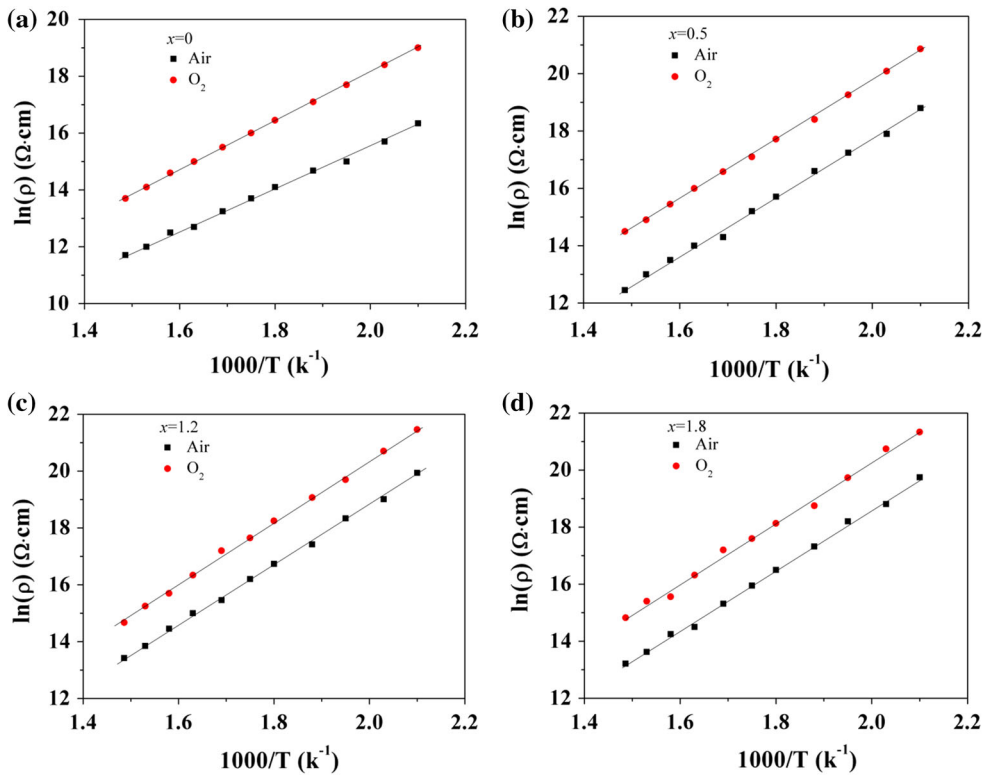

Fig. 6 Variation of ac conductivity for air and O_2 sintered BF–BT–*x* %Mn ceramics as a function of temperature

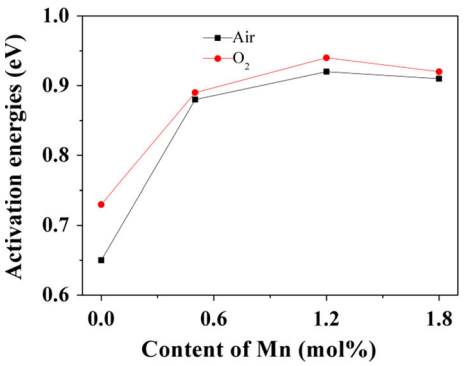

Fig. 7 The activation energies of BF–BT–*x* %Mn ceramics

shows a dramatic drop from about 0.15 to 0.07 at 100 Hz by sintering in O_2 atmosphere for BF–BT–0 %Mn ceramics. The *tanδ* of air sintered BF–BT–0.5 %Mn ceramics exhibits 0.058 at 100 Hz, when the ceramics sintered in O_2 atmosphere this value decreases to 0.046. When $x = 1.2$, the *tanδ* decreases from 0.043 to 0.036 at 100 Hz after sintering in O_2 atmosphere. All the O_2 sintered ceramics exhibit lower *tanδ* comparing to the air sintered especially at low frequency. This result shows that the defects of BF–BT–*x* %Mn ceramics are reduced by sintering in O_2 atmosphere.

Figure 4 presents the dielectric constant and loss of air and O_2 sintered BF–BT–*x* %Mn ceramics as a function of temperature at 10^6 Hz. All ceramics exhibit only a

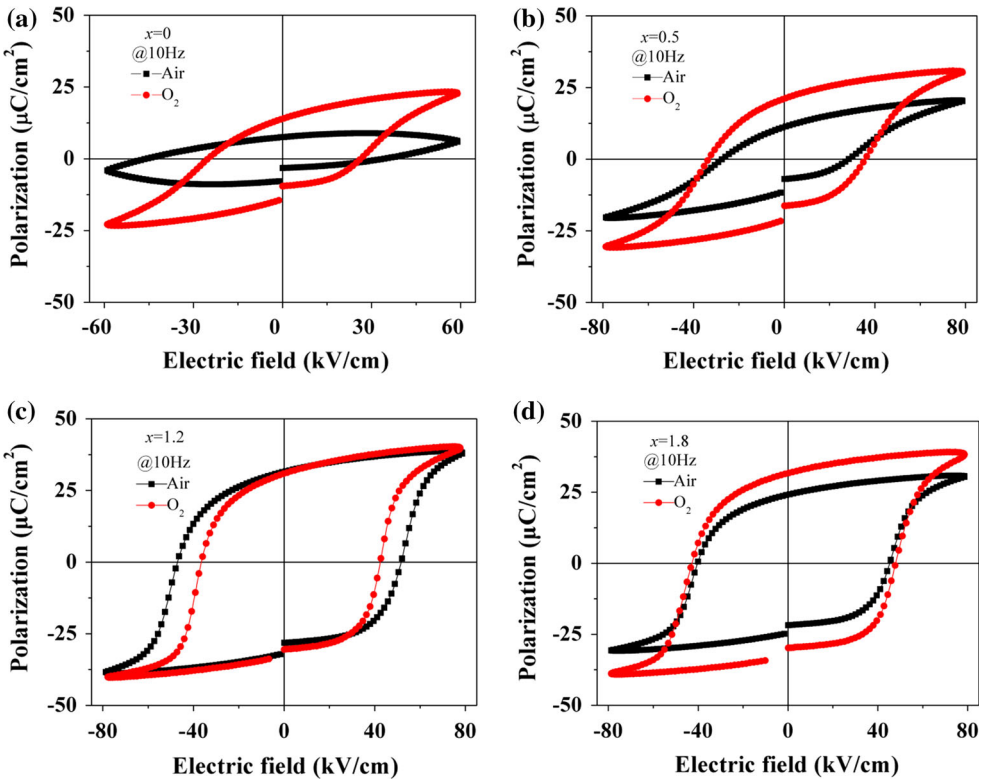

Fig. 8 *P–E* loops of BF–BT–*x* %Mn ceramics sintered at air and O_2 atmospheres

dielectric peak and the Curie temperature T_C determined by the dielectric peak is obtained. All O_2 sintered BF–BT–*x* %Mn ceramics almost keep the similar T_C with the air sintered ceramics. While the dielectric peak of O_2 sintered BF–BT–*x* %Mn ceramics is sharper than the air sintered. The O_2 sintered ceramics exhibit relatively small *tanδ* in high temperature, especially for BF–BT–0 %Mn ceramics. The *tanδ* of air sintered BF–BT–0 %Mn ceramics at 400 °C is 7.2 about 14 times that of the O_2 sintered ceramics. This phenomenon implies that the electric insulation of O_2 sintered in high temperature is better than the air sintered.

Figure 5 shows the impedance spectroscopy of BF–BT–*x* %Mn ceramics measured at 573 k. The impedance spectroscopy is characterized by the appearance of semicircular arcs, and the entire plots show single arc suggesting that the electrical process contribution is mainly from grain interior [11]. The total resistivity ρ of air sintered ceramics are increased with increasing the Mn content up to $x = 1.2$, subsequently decrease with increasing the Mn content. The ρ of O_2 sintered BF–BT–0 %Mn ceramics is 600 kΩ cm about 11 times that of the air sintered. The ρ of O_2 sintered BF–BT–0.5 %Mn ceramics is 2100 kΩ cm, 7.5 times that of the air sintered. The values of ρ for air and O_2 sintered BF–BT–1.2 %Mn ceramics are 700 and 3150 kΩ cm, respectively. This result suggests that the O_2 atmosphere can improve the insulation effectively, especially to the slightly Mn doping ceramics.

The variation of conductivity for air and O_2 sintered BF–BT–*x* %Mn ceramics as a function of temperature is exhibited in Fig. 6. With the temperature increases, the mobile charges have sufficient thermal energy to get activated and jump over the barrier. According to the Arrhenius relationship:

$$\sigma' = \sigma_0 \exp\left(\frac{-E_a}{k_B T}\right), \tag{1}$$

the activation energies for the BF–BT–*x* %Mn ceramics are estimated and exhibited in Fig. 7. The obtained activation energies for $x = 0$, 0.5, 1.2, 1.8 sintered in air were 0.65, 0.88, 0.92, 0.91 eV, respectively, indicating the ionic charge carriers may be the oxygen vacancies [12]. The activation energies of O_2 sintered ceramics increase firstly and then decrease with increasing the Mn content, reaching the maximum value 0.94 eV with $x = 1.2$. The activation energy of O_2 sintered BF–BT–0 %Mn ceramics is 0.73 eV, 0.8 eV larger than the air sintered one. According to the Kroger–Vink notation [13], the conduction electrons may be created by the following reactions:

$$O_O^x \rightarrow \frac{1}{2}O_2(g) + V_O^x \tag{2}$$

$$V_O^x \rightarrow V^* + e' \tag{3}$$

$$V_O^* \leftrightarrow V_O^{**} + e', \tag{4}$$

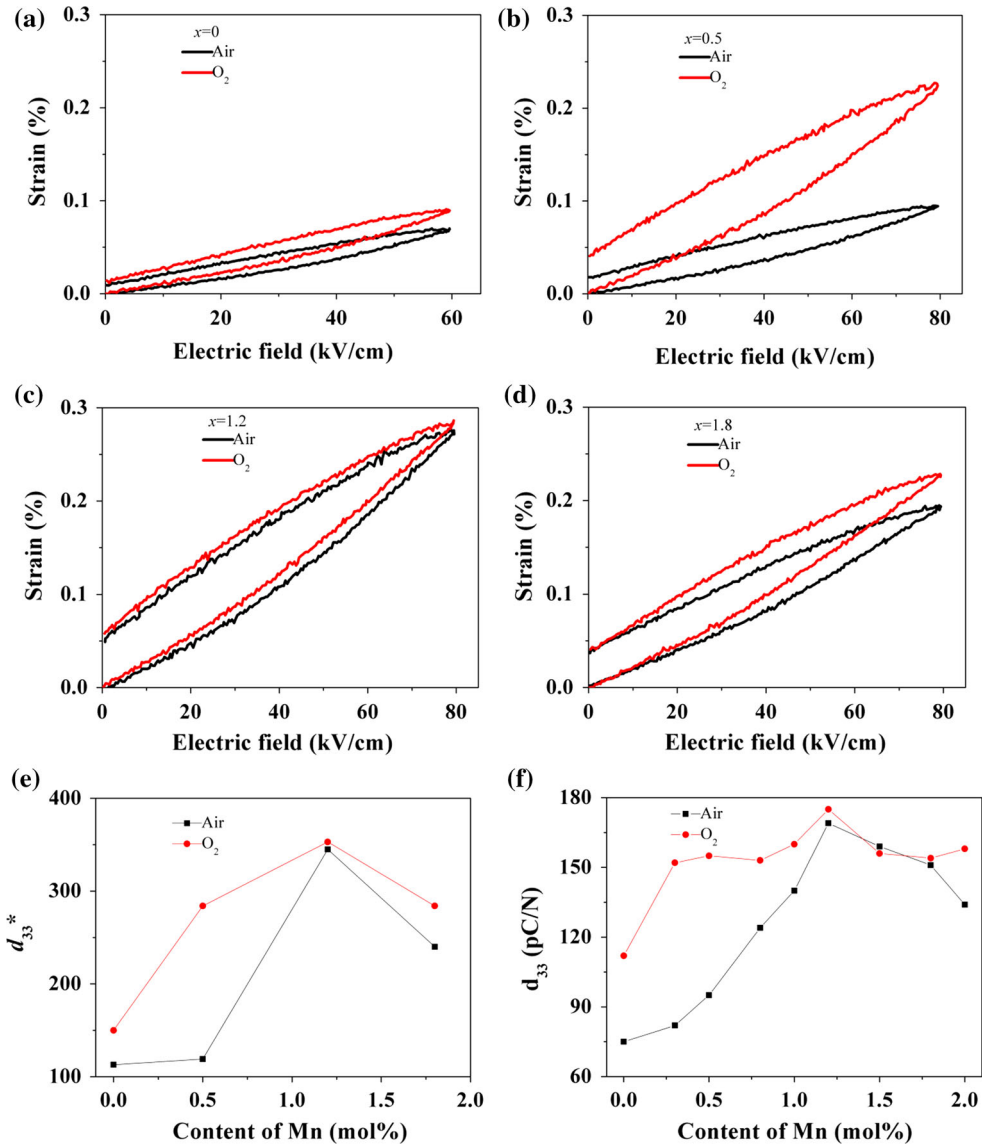

Fig. 9 Piezoelectric properties of BF–BT–*x* %Mn ceramics sintered in air and O_2 atmospheres

with increases the temperature, the electrons trapped by Ti^{4+} or Mn^{3+} ions [14] or oxygen vacancies are thermally activated, resulting in the decreasing of resistance. Therefore, the ceramics exhibit larger activation energy meaning that the ceramics possess lesser defects. The variation of activation energies for air and O_2 sintered ceramics shows that the O_2 atmosphere can reduce the defects effectively, meanwhile, the effects of sintering atmosphere on resistivity for BF–BT–*x* %Mn ceramics lie on the Mn content.

Figure 8 exhibits the room temperature *P*–*E* loops of the BF–BT–*x* %Mn ceramics sintered in air and O_2 atmospheres. The remnant polarization P_r of O_2 sintered BF–BT–0 %Mn ceramics is 14 μC/cm^2, while only 7.5 μC/cm^2 obtained from the air sintered. The observed P_r of BF–BT–0.8 %Mn ceramics increases from 11 to 21 μC/cm^2 when the sintering atmospheres change from air to O_2. The value of P_r for BF–BT–1.8 %Mn ceramics is also enhanced by sintered in O_2 atmosphere. According to the results of impedance spectroscopy analysis, it is possible that the freely movable charges may contribute to the electrical hysteresis loop for air sintered BF–BT–0 %Mn ceramics, characterized by the rounded features of the loop. Yet, the less rounded features of the loops show that the contribution to the polarization from the freely movable charges is reduced for O_2 sintered BF–BT–0 %Mn ceramics. The enhancement of insulation for O_2 sintered ceramics caused by the reduced oxygen vacancies makes it more possible to completely pole the ceramics, and thus the larger remnant polarization P_r may be obtained. Furthermore, the O_2 sintered ceramics possess larger and better interlinked grains and better grain boundary junction observed in Fig. 2, which may contribute to percolating inter-grain transport current and favor inhibiting the leakage current and hence

improve the electric polarization [15]. The BF–BT–1.2 %Mn ceramics exhibit almost the same P_r no matter ceramics sintered in air and O_2 atmospheres. These results suggest that the effects of sintering atmosphere on ferroelectric properties for BF–BT–x %Mn ceramics depend on the concentration of Mn doping.

The piezoelectric properties of BF–BT–x %Mn ceramics are shown in Fig. 9. Figure 9a–d show the unipolar curves at room temperature of BF–BT–x %Mn ceramics sintered in air and O_2 atmospheres. The strains of BF–BT–0 %Mn ceramics are enhanced from 0.07 to 0.09, meanwhile, the strains of BF–BT–0.5 %Mn increase from 0.09 to 0.22 after sintering in O_2 atmosphere. The strain of BF–BT–1.2 %Mn is 0.28, showing good piezoelectric properties. The piezoelectric constants d_{33}^*exhibited in Fig. 9e are calculated from Fig. 9a–d. It is notable that the d_{33}^* of BF–BT–0.5 %Mn ceramics increases from 119 to 284 pm/V and the d_{33}^* of O_2 sintered BF–BT–1.2 %Mn reaches to 353 pm/V. The piezoelectric constants d_{33} of all BF–BT–x %Mn ceramics sintered in air and O_2 atmospheres are exhibited in Fig. 9f. The observed d_{33} of air sintered $x = 0$, 0.3, 0.5, 0.8 ceramics are 75, 82, 95, 124 pC/N, respectively. After sintering in O_2 atmosphere, the d_{33} of $x = 0$, 0.3, 0.5, 0.8 ceramics are 112, 152, 155, 153 pC/N, showing great enhancement. These results imply that the O_2 atmosphere plays a crucial role in enhancing the piezoelectric properties of BF–BT–x %Mn ceramics especially to the slightly Mn doping. It is reported that the piezoelectric properties of the polycrystalline ceramics materials are mainly affected by the intrinsic and extrinsic factors [16]. The grain size is one of the important aspects to affect the extrinsic factor of ceramics which is contributed to piezoelectric properties. Therefore, the improvement piezoelectric properties may due to the increasing grain size and enhanced electrical insulation.

4 Conclusion

$0.71BiFeO_3$–$0.29BaTiO_3$ piezoelectric ceramics with Mn modification (BF–BT–x %Mn) sintered in air and O_2 atmosphere were fabricated by conventional solid state reaction method. The grain sizes of O_2 sintered ceramics were more homogeneous and larger. The impedance spectroscopy results showed that the O_2 atmosphere could effectively decrease the oxygen vacancies. The dielectric loss of O_2 sintered BF–BT–x %Mn ceramics at room temperature decreased obviously. Meanwhile, the electric insulation of ceramics in high temperature was improved with sintered in O_2 atmosphere. The ferroelectric and piezoelectric properties were improved by sintering in O_2 atmosphere. By sintering in O_2 atmosphere the strains of BF–BT–0.5 %Mn increased 2.5 times and the d_{33}^* increased from 119 to 284 pm/V. Thus, the O_2 atmosphere not only reduced defects but enhanced the ferroelectric and piezoelectric properties especially to the ceramics with slightly Mn doping. This work suggested that sintering in O_2 atmosphere was an useful method to reduce defects and enhance the dielectric, ferroelectric and piezoelectric properties. The O_2 sintered BF–BT–x %Mn ceramics shows promising candidate for high temperature piezoelectric applications.

References

1. Z. Cen, C. Zhou, H. Yang, Q. Zhou, W. Li, C. Yuan, J. Mater. Sci.: Mater. Electron. **24**(10), 3952–3957 (2013)
2. S.O. Leontsev, R.E. Eitel, J. Am. Ceram. Soc. **92**(12), 2957–2961 (2009)
3. S. Hunpratub, P. Thongbai, T. Yamwong, R. Yimnirun, S. Maensiri, J. Supercond. Nov. Magn. **25**(5), 1619–1622 (2012)
4. A.Z. Simões, C.S. Riccardi, M.L. Dos Santos, F.G. Garcia, E. Longo, J.A. Varela, Mater. Res. Bull. **44**(8), 1747–1752 (2009)
5. J.R. Cheng, N. Li, L.E. Cross, J. Appl. Phys. **94**, 5153–5157 (2003)
6. X.H. Liu, Z. Xu, S.B. Qu, X.Y. Wei, J.L. Chen, Ceram. Int. **34**(4), 797–801 (2008)
7. N. Itoh, T. Shimura, W. Sakamoto, T. Yogo, Ferroelectr **356**(1), 19–23 (2007)
8. Z. Yao, C. Xu, H. Hao, Q. Xu, W. Hu, M. Cao, H. Liu, Int. J. Appl. Ceram. Tec. **13**, 549–553 (2016)
9. W.M. Zhu, Z.G. Ye, Ceram. Int. **30**(7), 1435–1442 (2004)
10. Q. Hang, Z. Xing, X. Zhu, M. Yu, Y. Song, J. Zhu, Z. Liu, Ceram. Int. **38**, S411–S414 (2012)
11. H. Zhang, P. Xu, E. Patterson, J. Zang, S. Jiang, J. Rodel, J. Eur. Ceram. Soc. **35**(9), 2501–2512 (2015)
12. A. Munpakdee, K. Pengpat, J. Tontrakoon, T. Tunkasiri, Smart Mater. Struct. **15**(5), 1255 (2006)
13. S.P.S. Badwal, *Processing of the International Seminar on Solid State Ionic Devices* (World Scientific Publishing, Singapore, 1988), p. 165
14. P. Dhak, D. Dhak, M. Das, K. Pramanik, P. Pramanik, Mater. Sci. Eng. B **164**(3), 165–171 (2009)
15. S.K. Pradhan, B.K. Roul, Phys. B **407**(13), 2527–2532 (2012)
16. C.A. Randall, N. Kim, J.P. Kucera, W. Cao, T.R. Shrout, J. Am. Ceram. Soc. **81**(3), 677–688 (1998)